JOC Article

# Modeling the Effect of Substitution on the $Pb(OAc)_4$ Mediated Oxidative Cleavage of Steroidal 1,2-Diols

C. Öztürk, K. Topal, and V. Aviyente*

*Chemistry Department, Boğaziçi University 34342, Bebek, Istanbul, Turkey*

Nurcan Ş. Tüzün

*Chemistry Department, Istanbul Technical University, 34390, Maslak-Istanbul, Turkey*

E. Sánchez Fernández and S. Arseniyadis*

*Institut de Chimie des Substances Naturelles, CNRS, F-91198 Gif-sur-Yvette, France*

*aviye@boun.edu.tr; simeon.arseniyadis@icsn.cnrs-gif.fr*

*Received March 19, 2005*

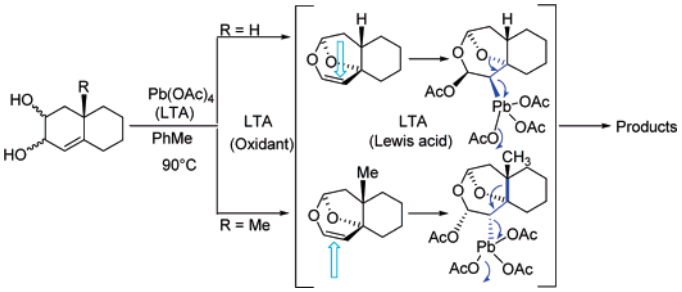


We comment on the effects of angular substitution on the outcome of a $Pb(OAc)_4$ (LTA) mediated heterodomino reaction, with selected bicyclic unsaturated 1,2-diols, which is considered to proceed through a series of transformations in a single vessel. The first two, oxidative and pericyclic, are followed by the key step, an electrophilic addition of LTA to the olefin, responsible for the course of the domino process. In this study, the electrophilic addition of LTA to the double bond has been modeled with B3LYP, where the 6-31G* basis set is used for C, O, and H atoms and the LANL2DZ method is used for Pb. The modeling in the gaseous phase and in solution has revealed the concerted nature of the addition of LTA to the double bond of the intermediate. The fact that LTA adds from the same side as the substituent R, for R=H and from the opposite side when $R=CH_3$ has been attributed to steric hindrance, which causes deformation of the olefinic intermediate.

## Introduction

We recently reported that unsaturated diols can react with the oxidant in several ways depending on the reaction conditions, the solvent,[1] the oxidant,[2] and the substitution pattern.[3] We provided experimental evidence that these factors can modify the behavior of the transient intermediates in domino reaction.[4] The reaction is dependent on the developing stereochemistry within the transient organolead intermediate, as the path followed after the electrophilic attack on the olefin in the angularly substituted series is at variance with that of the one followed in the nor-series. In line with our previous work, it was considered important to study the effect of angular substitution on the "path selectivity" of the domino reaction. On the basis of the proposed mechanistic pathway,[5] we hypothesized that the domino process could

(1) Candela Lena, J. I.; Sesenoglu, Ö.; Birlirakis, N.; Arseniyadis, S. *Tetrahedron Lett.* **2001**, *42*, 21−24.

(2) (a) Candela Lena, J. I.; Martín Hernando, J. I.; Rico Ferreira, M. R.; Altınel, E.; Arseniyadis, S. *Synlett* **2001**, 597−600. (b) Candela Lena, J. I.; Sánchez Fernández, E. M.; Ramani, A.; Birlirakis, N.; Barrero, A. F.; Arseniyadis, S. *Eur. J. Org. Chem.* **2005**, 683−700.

(3) Candela Lena, J. I.; Altınel, E.; Birlirakis, N.; Arseniyadis, S. *Tetrahedron Lett.* **2002**, *43*, 1409−1412.

(4) (a) Tietze, L. F.; Beifuss, U. *Angew. Chem., Int. Ed. Engl.* **1993**, *32*, 131−163. (b) Tietze, L. F. *Chem. Rev.* **1996**, *96*, 115−136. (c) Tietze, L. F.; Modi, A. *Med. Res. Rev.* **2000**, *20*, 304−322. (d) Tietze, L. F.; Haunert, F. In *Stimulating Concepts in Chemistry*; Shibasaki, M., Stoddart, J. F., Vogtle, F., Eds.; Wiley-VCH: Weinheim, Germany, 2000; pp 39−64.

(5) (a) Unaleroglu, C.; Aviyente, V.; Arseniyadis, S. *J. Org. Chem.* **2002**, *67*, 2447−2452. (b) Finet, L.; Candela Lena, J. I.; Kaoudi, T.; Birlirakis, N.; Arseniyadis, S. *Chem.−Eur. J.* **2003**, *9*, 3813−3820.

10.1021/jo0505627 CCC: $30.25 
Published on Web 08/09/2005

**SCHEME 1. Modulation of the Domino Process by the Substitution Pattern**

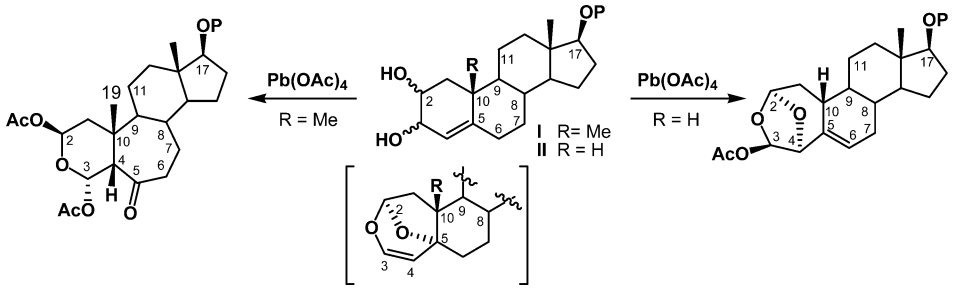


**SCHEME 2**[a]

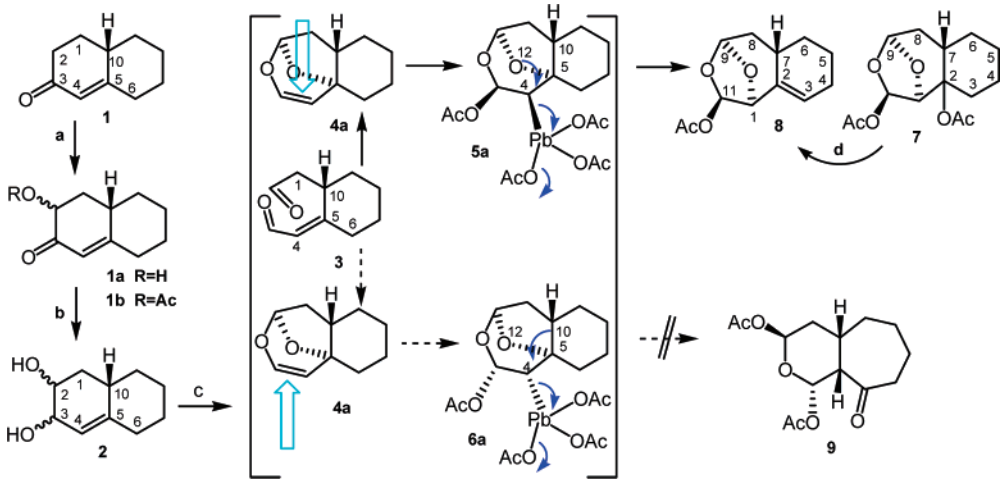


[a] (a) 4 equiv of $Pb(OAc)_4$, PhH, 90 °C, 3 days (75%). (b) $LiAlH_4-Et_2O$, 0 °C, 30 min. (88%). (c) 2.4 equiv of $Pb(OAc)_4$ in dry PhMe, 90 °C, 6 h. (d) PhMe, reflux, 3 h.

be modulated by the substitution pattern because the direction of metal attack on the olefin is likely to be governed by steric factors. To verify this hypothesis, we should create conditions to favor $\beta$-face attack of the metal to the olefin, for example, by removing the angular methyl substituent, as in 19-nor-testosterone derived unsaturated diols. A series of experiments addressed to the influence of substitution pattern during the domino transformations revealed that the path could be predictably determined by the geometry in the transient organolead intermediates (bond alignment factor), which in turn depends on the substitution pattern of the substrates investigated. Thus, lack of angular methyl substitution at C-10 led to a different domino process in agreement with the influence of the bond alignment of the migrating and leaving groups (C10−C5 migration, versus O12−C5 migration). Original experiments to probe the influence of the substitution pattern in the domino process are portrayed in Scheme 1.[6]

Although the rearrangement mechanism that we have proposed to account for the formation of the alternative cascade product **8** (Scheme 2) seems intuitively reasonable, it was considered desirable to quantify the energetics of the process, particularly in view of its importance as the basis for our assessment of the facial selectivity of metal attack. To do this, a model compound **2** was synthesized starting from the known $^{\Delta 1,9}$-octalone-2[7] **1** and subjected to our domino conditions. In our previous computational study,[5a] the two cascade-type transformations in the Hajos−Parrish and the Wieland−Miescher series have been modeled and found to yield structurally different products despite the similarities in the starting compounds which differ only by the number of carbon atoms in the cycloalkane rings. The diverging behavior in the mechanism of the interconversion has been attributed to the stabilization of a positive center by a carbonyl oxygen due to the flexibility of the seven-membered ring in contrast to the rigidity of the six-membered ring. In this study, the electrophilic addition of LTA to the half-cascade product **4** (**4a**: 9,12-dioxa-tricyclo[6.3.1.0 $^{0,0}$]dodec-10-ene- for R=H; **4b**: 6-methyl-9,12-dioxa-tricyclo[6.3.1.0 $^{0,0}$]dodec-10-ene for R=$CH_3$) has been modeled. The motivation of the computational modeling was to understand the mode of addition of LTA to compound **4** (**4a** for R=H, **4b** for R=$CH_3$) as well as to rationalize the effect of angular substitution on product distribution (Scheme 2).

## Computational Methodology

Preliminary examination of the reaction profile was carried with the PM3 method. The geometries have been fully optimized. Conformational searches around single bonds have been performed. Harmonic frequencies have been computed to identify the stationary points as minima (with all real

(6) (a) Martín Hernando, J. I.; Rico Ferreira, M.; Candela Lena, J. I.; Toupet, L.; Birlirakis, N.; Arseniyadis, S. *Tetrahedron: Asymmetry* **1999**, *10*, 3977−3989. (b) Del Rosario, M.; Ferreira, R.; Martín Hernando, J. I.; Candela Lena, J. I.; Toupet, L.; Birlirakis, N.; Arseniyadis, S. *Tetrahedron Lett.* **1999**, *40*, 7679−7682.

(7) Augustine, R. L.; Caputo, J. A. *Organic Syntheses*; Wiley & Sons: New York, 1973; Vol. V, p 869.

**SCHEME 3. Numbering System Used in the Text**

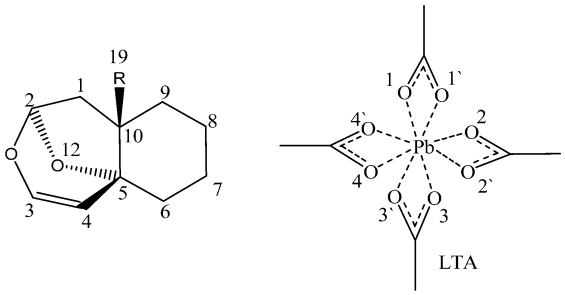


frequencies) or transition states (with only one imaginary frequency). The stationary points located with PM3 have been further optimized with B3LYP, where the 6-31G* basis set is used for C, O, and H atoms and the Los Alamos effective core potential plus double zeta (LANL2DZ) method is used for Pb. All calculations have been carried out with the Gaussian 98 program.[8] Among the effective core potential (ECP) methods, LANL2DZ is known to better approximate the experimental values when compared to the other two basis sets, namely SDD and LANL2MB.[9] The numbering system used in the text is shown in Scheme 3.

Solvent effects were modeled using the polarized continuum model (PCM) of Tomasi et al.[10] within self-consistent reaction field (SCRF) theory, by means of single-point calculations based on the gas-phase geometries. PCM has been developed to describe the solvent reaction field through the use of cavities of general shape, modeled on the solute. The cavity is built as the envelope of spheres centered on solute atoms or atomic groups (usually hydrogen atoms are included in the same sphere as the heavy atoms they are bonded to). The reaction field is described by means of apparent charges (solvation charges) spread on the cavity surface, designed to reproduce the electrostatic potential due to the polarized dielectric inside the cavity. Such charges are used both to compute solute−solvent interactions (modifying the total energy of the solute) and to perturb the molecular Hamiltonian through a suitable operator (thus distorting the solute wave function and affecting all the electronic properties).

## Results and Discussion

**Preparation of the Domino Precursor.** For the preparation of the bicyclic unsaturated 1,2-diol **2**, the requisite domino substrate, the well-known Robinson annulation procedure as described by Augustine was used, starting from 1,3-cyclohexanedione and methyl vinyl ketone.[7] The bicyclic enone **1** thus obtained was

**SCHEME 4. Top and Bottom Face Attack of LTA**

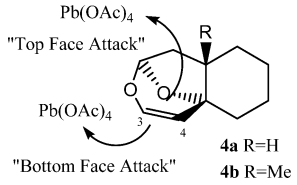


acetoxylated by LTA in benzene at reflux, under Dean−Stark conditions for water removal affording **1b**.[11] The diol was then obtained by lithium aluminum hydride reduction in ether at 0 °C, as a diastereomeric mixture, and used as such since LTA mediated oxidative cleavage[12] is effective irrespective of the diol stereochemistry. The latter is a very effective cleavage agent of diols, but it is also capable of adding to an olefin and then deplumbylating.[13]

A mechanism that explains the conversion of **2** to **8** is shown in Scheme 2. Upon treatment with LTA, **2** initially undergoes an oxidative cleavage to the dialdehyde **3** followed by a 4 + 2 cycloaddition leading to **4a**. The latter upon further reaction with LTA could form an organolead intermediate of either type **5a** or **6a**, which in turn should undergo rearrangement to afford **7** or **9**, respectively. Ring expansion leading to **9** requires alignment of the C4−Pb bond with the C10−C5 bond. An alternative transformation leading to **7** (and hence to **8**) would require alignment of the C4−Pb bond with the C5−O12 bond involving 1,2-oxygen shift of the best aligned C5−O12 bond. Consideration of the pathway shown in Scheme 2 suggests that **7** and **8** are derived from the transient organolead intermediate **5a**. An "alternative" fragmentation represented by the blue arrows in structure **5a** intervened to give products lacking the ring-enlargement (blue arrows in **6a**). The first bond migration that connects O12 with C4 occurs rapidly due to favorable orbital alignment, and subsequent trapping of the resultant bridgehead cation at C2 by the acetate leads to **7** and **8**. The latter results from the initially formed **7** via a loss of acetic acid unit. Upon heating in toluene, **7** is smoothly converted to **8**. The outcome of LTA mediated domino reactions depends originally on steric factors, which in turn control the effectiveness of orbital overlap depending on the initial alignment of relevant bonds. In the above proposed rearrangements, the migrating bond has to be antiperiplanar to the leaving group ("$sp^3$ alignment factor"). Addition of LTA to the C3−C4 double bond of the intermediate **4** proceeds from the top face ($\beta$ face) in the case where the substituent R on the bridgehead carbon, C10, is H (R=H); the attack takes place from the bottom face ($\alpha$ face), when R=$CH_3$ as portrayed in Scheme 4.

(8) Frisch, M. J.; Trucks, G. W.; Schlegel, H. B.; Scuseria, G. E.; Robb, M. A.; Cheeseman, J. R.; Zakrzewski, V. G. Montgomery, J. A., Jr.; Stratmann, R. E.; Burant, J. C.; Dapprich, S.; Millam, J. M.; Daniels, A. D.; Kudin, K. N.; Strain, M. C.; Farkas, O.; Tomasi, J.; Barone, V.; Cossi, M.; Cammi, R.; Mennucci, B.; Pomelli, C.; Adamo, C.; Clifford, S.; Ochterski, J.; Petersson, G. A.; Ayala, P. Y.; Cui, Q.; Morokuma, K.; Malick, D. K.; Rabuck, A. D.; Raghavachari, K.; Foresman, J. B.; Cioslowski, J.; Ortiz, J. V.; Stefanov, B. B.; Liu, G.; Liashenko, A.; Piskorz, P.; Komaromi, I.; Gomperts, R.; Martin, R. L.; Fox, D. J.; Keith, T.; Al-Laham, M. A.; Peng, C. Y.; Nanayakkara, A.; Gonzalez, C.; Challacombe, M.; Gill, P. M. W.; Johnson, B. G.; Chen, W.; Wong, M. W.; Andres, J. L.; Head-Gordon, M.; Replogle, E. S.; Pople, J. A. *Gaussian 98*, revision A.11.1; Gaussian, Inc.: Pittsburgh, PA, 1998.

(9) (a) Zhao, J.; Zhang, Y.; Kan, Y.; Zhu, L. *Spectrochim. Acta, Part A* **2004**, *60*, 679−688. (b) Hay, P. J.; Wadt, W. R. *J. Chem. Phys*. **1985**, *82*, 270−283. (c) Wadt, W. R.; Hay, P. J. *J. Chem. Phys*. **1985**, *82*, 284−298. (d) Hay, P. J.; Wadt, W. R. *J. Chem. Phys.* **1985**, *82*, 299−310.

(10) (a) Mennucci, B.; Tomasi, J. *J. Chem. Phys.* **1997**, *106*, 5151−5158. (b) Mennucci, B.; Cancès, E.; Tomasi, J. *J. Phys. Chem. B* **1997**, *101*, 10506−10517. (c) Cammi, R.; Mennucci, B.; Tomasi, J. *J. Phys. Chem. A* **1999**, *103*, 9100−9108. (d) Cammi, R.; Mennucci, B.; Tomasi, J. *J. Phys. Chem. A* **2000**, *104*, 5631−5637.

(11) (a) Arseniyadis, S.; Rodriguez, R.; Muñoz Dorado, M.; Brondi Alves, R.; Ouazzani, J.; Ourisson, G. *Tetrahedron* **1994**, *50*, 8399−8426. (b) Arseniyadis, S.; Rodriguez, R.; Brondi, R.; Spanevello, R.; Ouazzani, J.; Ourisson, G. *NATO ASI Ser., Ser. C* **1992**, *381*, 313−321.

(12) The corresponding saturated bicyclic diols, upon treatment with the oxidant, led to the expected dialdehyde resulting from a glycol fission while inserting an olefin into the bicyclic ring system, completely modifying the reaction outcome. (a) Criegee, R. *Chem. Ber.* **1931**, *64*, 260−266. (b) Criegee, R.; Beucker, H. *Ann. Chem.* **1939**, *541*, 218. (c) Criegee, R. In *Oxidation in Organic Chemistry, Part A*; Wiberg, K. B., Ed.; Academic Press: New York, 1965; p 277.

(13) Arseniyadis, S.; Brondi Alves, R.; Pereira de Freitas, R.; Muñoz-Dorado, M.; Yashunsky, D. V.; Potier, P.; Toupet, L. *Heterocycles* **1997**, *46*, 727−764.

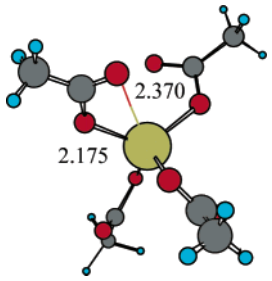


**FIGURE 1.** Structure of LTA (B3LYP/6-31G* (LANL2DZ on Pb)).

**TABLE 1. X-ray Crystallographic Data (Å) of LTA**

| | |
|---|---|
| Pb−O1 | 2.278 |
| Pb−O1′ | 2.249 |
| Pb−O2 | 2.287 |
| Pb−O2′ | 2.268 |
| Pb−O3 | 2.253 |
| Pb−O3′ | 2.312 |
| Pb−O4 | 2.292 |
| Pb−O4′ | 2.255 |

**SCHEME 5. Hypothetical $S_N2$ Mechanism for LTA Addition to 4a and 4b**

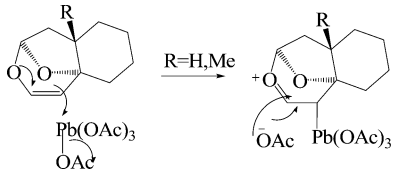


**Structure of LTA.** The structure of LTA where the acetate groups are bidentate has been modeled with B3LYP/6-31G* (LANL2DZ on Pb). The structure of LTA is such that the oxygen atoms of the acetate group face the central atom, Pb. In each acetate group one O is 2.175 Å, the other is 2.370 Å away from Pb. Thus, among the eight O atoms, four are at 2.175 Å and the other four are at 2.370 Å from the central atom. In the X-ray crystallographic data the structure of LTA is seen to consist of two discrete molecules in each of which the Pb atom is surrounded by four bidentate acetate ligands forming a nearly dodecahedral polyhedron.[14] The calculated geometrical parameters in Figure 1 are similar to those in Table 1.

The first approach to the problem was to model an $S_N2$-type reaction where one of the OAc groups leaves while Pb attacks the double bond. This strategy has been repeated several times for different orientations of $Pb(OAc)_4$ with respect to the double bond (Scheme 5). No stationary structures have been located along this type of approach. If an $S_N2$ mechanism were to be suggested, when LTA adds to the double bond via a ligand exchange mechanism where the bicyclic diol molecule replaces one of the acetate groups of LTA, the carbocation would have a quasi-planar structure. In that case, the nucleophilic $OAc^-$ would have the opportunity to attack the carbocation from both sides. This type of mechanism could considerably reduce the selectivity.

We have then suggested a concerted addition mechanism (Scheme 6). There is strong experimental evidence

(14) Schürmann, M.; Huber, F. *Acta Crystallogr., Sect. C* **1994**, *50*, 1710−1713.

**SCHEME 6. Reaction Path**

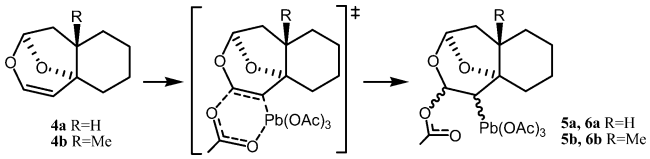


**TABLE 2. Total Electronic Energies (hartrees) in Parentheses and Relative Energies (kcal/mol) of the Transition Structures (B3LYP) in Vacuum ($\epsilon = 1$) and in Toluene ($\epsilon = 2.24$)**

| | 6-31G* (LANL2DZ on Pb) ($\epsilon = 1$) | | 6-31+G*//6-31G* (LANL2DZ on Pb) ($\epsilon = 2.24$) |
|---|---|---|---|
| **HA** | (−1456.922739) | **0.00** | **0.00** |
| **HB** | (−1456.918031) | 2.95 | 2.29 |
| **MA** | (−1496.197543) | 1.72 | 0.77 |
| **MB** | (−1496.200271) | **0.00** | **0.00** |

that even in acetic acid the acetate group that adds to the substrate is the one that belongs to LTA.[15] The selectivity of the reaction will depend on the relative energies of the transition structures where LTA attacks the intermediate (**4a** or **4b**) from the same side (above) or opposite side (below) of "R" as shown in Scheme 4.

Four different cases have been considered:

(1) Electrophilic attack of LTA to compound **4a** from the same direction as R for R=H. The corresponding transition structure for this attack has been denoted as **HA**.

(2) Electrophilic attack of LTA to compound **4a** from the direction opposite to R for R=H. The corresponding transition structure for this attack has been denoted as **HB**.

(3) Electrophilic attack of LTA to compound **4b** from the same direction as R for $R=CH_3$. The corresponding transition structure for this attack has been denoted as **MA**.

(4) Electrophilic attack of LTA to compound **4b** from the direction opposite to R for $R=CH_3$. The corresponding transition structure for this attack has been denoted as **MB**.

The total electronic energies (B3LYP/6-31G* and LANL2DZ on Pb) with zero-point energy included indicate that for R=H the attack from the top face is approximately 140 times faster than the attack from the bottom face in a vacuum (Table 2). On the other hand, for $R=CH_3$ the attack from the bottom face is almost 18 times faster than the one from the top face in the gas phase.

**Effect of the Media on the Selectivity.** Single-point energies in toluene (B3LYP/6-31+G*//6-31G* ($\epsilon = 2.24$)) have shown the same trend to be reproduced in solution: for R=H the attack from the top face is 47 times faster than the one from the bottom, while for $R=CH_3$ the attack from the bottom face is 4 times faster than the attack from the top.

**Can $Pb(OAc)_4$ Dissociate before Attacking Compound 4?** The energetics of reactions 1 and 2 have been calculated in the experimental medium, toluene.

$$Pb(OAc)_4 \rightarrow Pb(OAc)_3^+ + OAc^- \quad (1)$$

$$Pb(OAc)_4 \rightarrow Pb(OAc)_3^{\bullet} + OAc^{\bullet} \quad (2)$$

The heat of reaction for the ionization of $Pb(OAc)_4$ based

**SCHEME 7. Structures for the Addition of LTA to Intermediate 4 (B3LYP)**

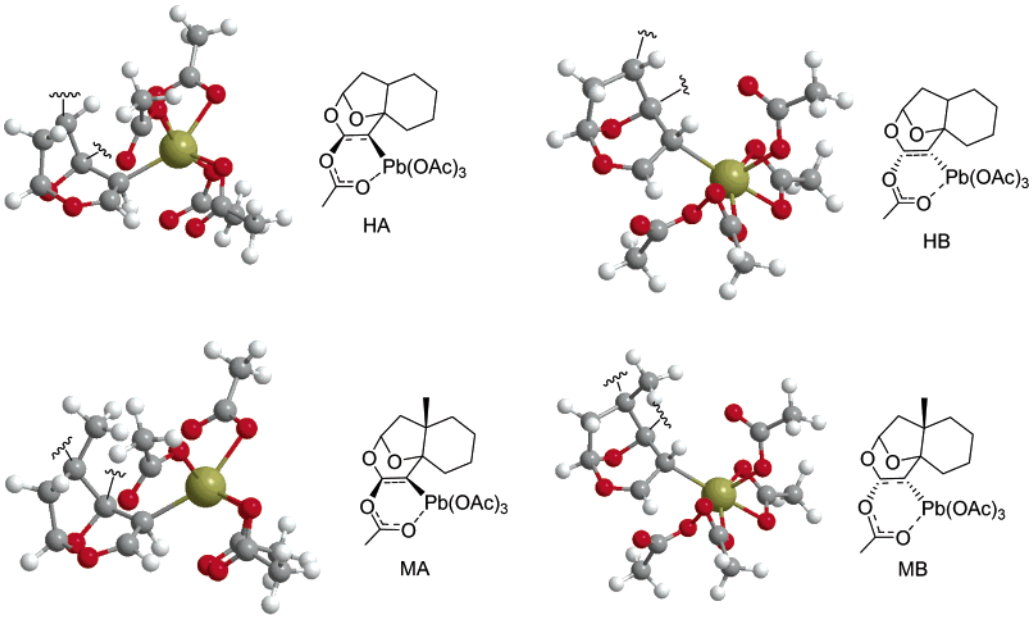


**TABLE 3. Critical Distances in the Transition States (B3LYP/6-31G* (LANL2DZ on Pb) ($\epsilon$ = 1))**

| | Pb−O1 | C3−O1′ |
|---|---|---|
| **HA** | 2.048 | 2.238 |
| **HB** | 2.192 | 2.178 |
| **MA** | 2.127 | 2.219 |
| **MB** | 2.146 | 2.187 |

**TABLE 4. Geometrical Parameters in Compounds 4a, 4b, HA, HB, MA, MB[a]**

| | **4a** | **4b** | **HA** | **HB** | **MA** | **MB** |
|---|---|---|---|---|---|---|
| C1−C2−O−C3 | −70.8 | −71.5 | −69.9 | −80.3 | −72.7 | −83.8 |
| C10−C5−C4−Pb | | | −65.0 | −146.3 | −74.9 | −148.7 |
| C10−C5−C6−C7 | −42.1 | −46.5 | −38.0 | −40.6 | −46.1 | −43.0 |
| Pb−C4−C3−O | | | 152.5 | −149.9 | 160.9 | −150.1 |
| C2−O−C3−C4 | −4.3 | −3.3 | −15.6 | 9.6 | −11.8 | 13.1 |
| Pb−C4−C5 | | | 119.2 | 120.4 | 126.4 | 120.4 |
| Pb−C4−C3 | | | 110.5 | 107.0 | 109.4 | 106.5 |
| C10−C5−C4 | 111.4 | 112.6 | 114.7 | 110.6 | 119.7 | 113.2 |
| C1−C2−O | 110.7 | 110.8 | 109.1 | 107. | 108.4 | 107.0 |
| C19−C10−C5 (H19−C10−C5) | 110.2 | 114.0 | 109.9 | 109.4 | 116.6 | 114.9 |

[a] (B3LYP/6-31G* (LANL2DZ on Pb) ($\epsilon$ = 1)).

on reaction 1 is 102.1 kcal/mol (PCM-B3LYP/6-31G*//B3LYP/6-31G*), and the homolytic cleavage of the two Pb−O bonds in $Pb(OAc)_4$ via reaction 2 is endothermic by 54.00 kcal/mol (PCM-B3LYP/6-31G*//B3LYP/6-31G*). On the basis of Hammond's postulate, the energy barriers for reactions 1 and 2 are expected to exceed 102.1 kcal/mol in the first case and 54.00 kcal/mol in the second case. These barriers are by far higher than the barriers for the attack of LTA to compounds **4a** and **4b**, which range between 35 and 40 kcal/mol with the same methodology (PCM-B3LYP/6-31G*//B3LYP/6-31G*). Thus, it is very improbable for $Pb(OAc)_4$ to decompose via reactions 1 or 2, leading to radicalic or cationic pathways, before attacking the substrate.

**Geometrical Parameters of the Transition Structures.** The 3D views of the transition structures are displayed in Scheme 7. The bond lengths for the acetate group departing Pb (Pb−O1′) and attacking the double bond (C3−O1′) in the transition states are given in Table 3. As expected, LTA is closer to the intermediate when it approaches from the opposite side to R: the forming C3−O1′ bond is shorter for **HB** and **MB**. On the other hand, in all cases the Pb−O distance is slightly shorter than it is in LTA.

**Top versus Bottom Side Attack.** The differences in energy barriers between the top face and bottom face attack have been rationalized with the B3LYP/6-31G* (LANL2DZ on Pb) methodology in the gas phase, by considering the presence of H bonds, the deformations in LTA, and the substrate in the transition structures. The number of stabilizing H-bonding interactions in **HA** and **MA** (around 10 in each) is equal to each other, the same is true for **HB** and **MB** (seven such interactions in each). Thus, the preference for the bottom face attack in the case of R=$CH_3$ cannot be accounted for, based on the presence of H-bonds.

Deformations in the transition structure of LTA for R=H and R=$CH_3$ have been monitored. The number of deformations in the LTA portion in **HA** (two of the Pb−O bonds have been elongated to 3.3 and 3.3 Å) is smaller than the one in **HB** (three of the Pb−O bonds have been elongated to 3.2, 3.2, and 3.0 Å). The number of deformations in the LTA portion in **MB** (two of the Pb−O bonds have been elongated to 3.4, 2.8, and 3.3 Å) is smaller than the one in **HB** (three of the Pb−O bonds have been elongated to 3.0, 3.1, and 3.2 Å). Overall, in **HB** and **MA** three bonds are longer than their corresponding homologues in LTA, whereas only two bonds have been elongated in the preferred transition structures **HA** and **MB**.

As seen in Table 4 for the "$\beta$" face attack of LTA, the dihedral angles of **HA** and **MA** are more or less similar to the ones in the intermediate, except for C2−O−C3−C4. Normally the "$\beta$" face attack (above) should have been

(15) Sesenoglu, Ö.; Candela Lena, J. I.; Altinel, E.; Birlirakis, N.; Arseniyadis, S. *Tetrahedron: Asymmetry* **2005**, *16*, 995−1015.

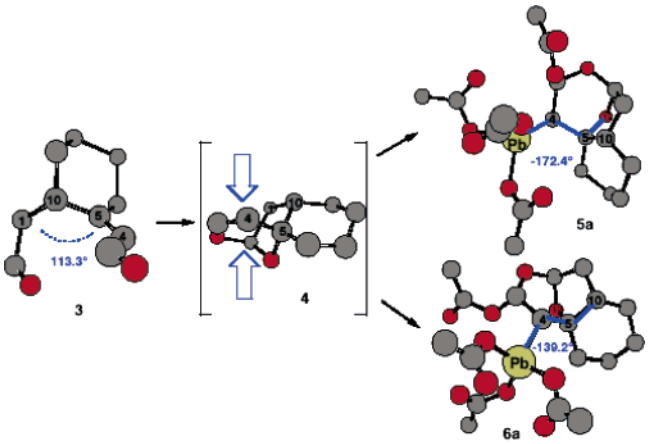


**FIGURE 2.** Influence of the substitution pattern rationalized in terms of the successive PM3 minimized structures for **3a**, **4a**, **5a**, and **6a**.

favored for R=H and R=$CH_3$. However, in the "$\beta$" face attack the C10−C5−C4 angle for **MA** alters from 112.6° to 119.7°. The hybridization of C5 switches from $sp^3$ in the intermediate (R=$CH_3$) to $sp^2$ in **MA**. This change in hybridization is possibly due to the steric repulsions between the methyl group at the angular position and LTA. The same carbon is quasi $sp^3$ in **HA**, and the approach of LTA has not modified the overall geometry of the substrate.

Furthermore, when the attack is from the bottom face the hybridization is similar in the substrates, **HB** and **MB**, respectively. Thus, in the case of R=$CH_3$, the substrate suffers from the top face attack and is distorted and **MA** is not preferred.

The influence of the substitution pattern is rationalized in terms of the successive PM3 minimized structures for **3**, **4a**, **5a**, and **6a** (Figure 2). The 3-D structures for compounds **5a** and **6a** have provided insight into the operation of an apparent stereoelectronic control in product distribution and is supportive of the mechanistic reasoning advanced in our earlier studies.[5] This can help in rationalizing, though qualitatively, the diverging behavior of the organolead intermediates **5a** and **6a**. Changing from methyl group to hydrogen at the angular position significantly decreases the rate of C10−C5 bond migration in **6a** while renders it unlikely in **5a**; the calculated dihedral angles are −60° and −139.2° (C10−C5−C4−Pb) for **5a** and **6a**, respectively. The latter is most likely formed to some extent but, unable to undergo ring expansion under the domino conditions, is destroyed. Conversely, the dihedral angle O12−C5−C4−Pb for **5a** being −172.4° allows for O12−C5 bond migration, thus leading to the only observed domino compound **7** and hence **8**.

## Conclusion

The LTA mediated domino reaction is remarkable since it relies on various separate steps occurring sequentially within a single reaction vessel. Additionally, the path can be predictably determined by geometry in the transient organolead intermediate, which in turn depends on the substitution pattern of the substrate investigated. The study of electrophilic addition of LTA to **4** in a vacuum has shown that the addition to the double bond is concerted. The fact that LTA adds from the same side as the substituent R for R=H and from the opposite side when R=$CH_3$ has been attributed to steric hindrance that causes deformation of the olefinic intermediate.

## Experimental Section

General experimental details were as previously described.[2b]

**Acetoxylation of Bicyclic Enone 1 with Pb(OAc)$_4$.** A dry three-necked flask, equipped with a Dean−Stark apparatus, was charged with **1** (1.91 g, 12.76 mmol) and $Pb(OAc)_4$ (22.62 g, 51.02 mmol, 4 equiv), vacuumed, and flushed with argon before dry benzene (80 mL) was added and the reaction mixture was heated at 90 °C (oil bath temperature should not exceed 100 °C) for 3 days. After cooling, a large volume of ether was added, and the reaction mixture was stirred for an additional hour and filtered. The filtrate was washed with brine and water, dried on $MgSO_4$, concentrated, and purified by chromatography on silica with heptane−EtOAc 5:1 as eluent, affording 1.99 g (75%) of the desired bicyclic acetoxy enones as a nearly 1:1 unseparable epimeric mixture which were taken as such for the next step.

**3-Oxo-1,2,3,5,6,7,8,8a-octahydronaphthallen-2-yl Acetate 1b:** IR (film): 2933, 2859, 1748, 1689, 1624, 1448, 1373, 1238, 1062, 917, 852 $cm^{-1}$. $^1H$ NMR (300 MHz): 1.09−2.59 (22H, m), 2.16 (3H, s), 2.17 (3H, s), 5.31 (1H, dd, $J$ = 7.9, 5.5), 5.34 (1H, dd, $J$ = 12.2, 6.0), 5.83 (1H, bs), 5.84 (1H, bs). $^{13}C$ NMR (75 MHz): 20.9 (2C), 25.1, 26.0 (2C), 26.4, 28.5, 33.3, 34.1, 34.6, 34.8, 36.5 (2C), 37.8, 38.4, 70.6, 72.8, 120.9, 122.7, 166.7, 168.2, 170.2, 193.9, 194.0. EIMS: 208 ($[M]^{+\bullet}$, 22), 148 (45), 122 (100), 94 (36), 79 (30).

For characterization purposes, the acetoxy enone **1b** was hydrolyzed by standard methods ($K_2CO_3$, MeOH−$H_2O$, 0 °C, 1 h) to its corresponding hydroxy enones. The diastereomeric mixture thus obtained was purified by silica gel flash column chromatography, using heptane−EtOAc, 1:1, as eluent.

**Faster Eluting Hydroxy Enone, 3-Hydroxy-4,4a,5,6,7,8-hexahydro-3H-naphthalen-2-one 1a (C-3 Configuration Unassigned):** IR (film): 3470, 2929, 2857, 1744, 1675, 1626, 1448, 1370, 1263, 1218, 1135, 1103, 1064, 895, 850 $cm^{-1}$. $^1H$ NMR (300 MHz): 1.20 (1H, m), 1.42 (1H, t, $J$ = 12.9), 1.30−1.52 (2H, m), 1.75−2.01 (3H, m), 2.20 (1H, m), 2.35 (1H, dd, $J$ = 12.9, 6.5), 2.48 (2H, m), 3.75 (1H, bs, OH), 4.10 (1H, dd, $J$ = 12.9, 6.5), 5.80 (1H, bs). $^{13}C$ NMR (75 MHz): 25.1, 26.4, 34.5, 34.9, 37.2, 37.6, 71.5, 120.1, 168.8, 200.0. ESIMS (MeOH): 167 ($[MH]^+$, 100), 189 ($[MNa]^+$, 18), 205($[MK]^+$, 4). HRESIMS: calcd for $C_{10}H_{14}O_2Na$ *m/z* 189.0891, found 189.0894.

**Reduction of the Acetoxy Enone 1b.** To a magnetically stirred suspension of $LiAlH_4$ (293 mg, 7.7 mmol) in 25 mL of anhydrous $Et_2O$, cooled to nearly 0 °C, was added dropwise a solution of the acetoxy enone (1.03 g, 6.17 mmol) in anhydrous ether (10 mL). After being stirred at this temperature for 30 min (TLC monitoring), the mixture was diluted with $Et_2O$ and treated with 0.3 mL of water, 0.3 mL of 6 N NaOH, and an additional 0.3 mL of water and stirred for 20 more minutes. The organic layer was dried with $MgSO_4$, concentrated at reduced pressure to give, after silica gel chromatography (eluent: EtOAc), 985 mg (88%) of the desired diols.

**1,2,3,5,6,8,8a-Octahydronaphthalene-2,3-diol 2 (One Dia Described, Stereochemistry Unassigned):** IR (film): 3368, 2925, 2852, 1665, 1445, 1233, 1252, 1053, 966, 851 $cm^{-1}$. $^1H$ NMR (300 MHz): 0.91−1.40 (4H, m), 1.68 (1H, m), 1.86−2.16 (4H, m), 3.20 (2H, OH), 3.80 (1H, m), 4.02 (1H, m), 5.19 (1H, m). $^{13}C$ NMR (75 MHz): 26.3, 27.9, 25.0, 33.6, 34.7 (C-10), 35.0, 67.2 (C-2), 67.7 (C-3), 118.9 (C-4), 145.0 (C-5). ESIMS (MeOH): 191 ($[MNa]^+$, 100). HRESIMS: calcd for $C_{10}H_{16}O_2Na$ *m/z* 191.1048, found 191.1042.

**Domino Reaction on the Octaline-diol 2.** A dry flask was charged with unsaturated diol **2** (550 mg, 3.27 mmol) and $Pb(OAc)_4$ (3.47 g, 7.85 mmol), vacuumed, and flushed with argon. Toluene (35 mL) was added, and the reaction mixture

was stirred for 6 h at 90 °C. The mixture was diluted with $Et_2O$ and filtered through a column containing Celite, $MgSO_4$, and $SiO_2$ with heptane−$Et_2O$, 1:1. The organic layer was concentrated under reduced pressure and purified through flash chromatography using heptane−EtOAc (1:1) as eluent, affording the dialdehyde **3** (321 mg, 59%), which is unstable, as the major component of a mixture of three compounds, the remaining two being **7** (56 mg, 6%) and its deacetylated counterpart **8** (190 mg, 26%).

**Acetic Acid 10,12-Dioxa-tricyclo[7.2.1.0$^{0,0}$]dodec-2-en-11-yl Ester 8:** mp: 56−58 °C (ether−heptane). IR (film): 2926, 2855, 1740, 1449, 1378, 1233, 1131, 1096, 1070, 1038, 994, 974, 935, 895, 853, 790 cm$^{-1}$. $^1$H NMR (300 MHz): 1.21 (1H, m, H-6), 1.46 (1H, m, H-8), 1.83 (3H, m, H-5, H-6), 2.03 (1H, dd, $J$ = 13.7, 7.2, H-8), 2.07 (3H, s, C$\underline{H}_3$CO), 2.08 (2H, m, H-4), 2.75 (1H, m, H-7), 4.60 (1H, d $J$ = 3.6, H-1), 5.56 (1H, s, H-9), 5.60 (1H, s, H-3), 6.05 (1H, d, $J$ = 3 0.6, H-11). $^{13}$C NMR (75 MHz): 20.9 ($CH_3$CO), 22.1 (C-5), 25.0 (C-4), 29.8 (C-7), 30.0 (C-6), 38.5 (C-8), 79.5 (C-1), 95.9 (C-11), 103.0 (C-9), 126.4 (C-3), 133.1 (C-2), 169.8 ($CH_3\underline{C}O$). ESIMS (MeOH): 263 ([MK]$^+$, 20), 247 ([MNa]$^+$, 100). HRESIMS: calcd for $C_{12}H_{16}O_4Na$ *m*/*z* 247.0946, found 247.0941.

**Acetic Acid 2-Acetoxy-10,12-dioxa-tricyclo[7.2.1.0$^{0,0}$]-dodec-11-yl Ester 7:** IR (film): 2931, 2860, 1747, 1452, 1369, 1247, 1167, 1124, 1109, 1039, 965, 937, 891, 793, 634, 602 cm$^{-1}$. $^1$H NMR (300 MHz): 1.28−1.42 (3H, m, H-3, H-4, H-6), 1.53 (1H, m, H-5), 1.59 (1H, m, H-5), 1.70 (1H, ddd, $J$ = 14.1, 6.3, 1.9, H-8), 1.90−2.02 (2H, m, H-4, H-6), 1.94 (1H, dd, $J$ = 14.1, 1.6, H-8), 2.03 (3H, s, C$\underline{H}_3$CO), 2.14 (3H, s, C$\underline{H}_3$CO), 2.54 (1H, m, H-3), 2.70 (1H, m, H-7), 5.20 (1H, d, $J$ = 4.2, H-1), 5.49 (1H, t, $J$ = 1.7, H-9), 6.17 (1H, d, $J$ = 4.2, H-11). $^{13}$C NMR (75 MHz): 20.2 (C-5), 20.9 ($\underline{C}H_3$CO), 21.0 (C-6), 21.7 ($\underline{C}H_3$CO), 25.3 (C-3), 26.2 (C-4), 31.9 (C-7), 33.6 (C-8), 74.3 (C-1), 80.9 (C-2), 96.0 (C-11), 103.0 (C-9), 169.5 ($CH_3\underline{C}O$), 169.9 ($CH_3\underline{C}O$). ESIMS (MeOH): 323 ([MK]$^+$, 20), 307 ([MNa]$^+$, 100). HRESIMS: calcd for $C_{14}H_{20}O_6Na$ *m*/*z* 307.1157, found 307.1150.

**Acknowledgment.** We thank the Bogazici University Research Foundation for financial support. Part of the computation for the work described in this article was supported by TUBITAK ULAKBIM High Performance Computing Center.

**Supporting Information Available:** Cartesian coordinates, energetics, and imaginary frequencies. This material is available free of charge via the Internet at http://pubs.acs.org.

JO0505627